

## Supporting Information

### Performance of Nano-Assembly Logic Gates with a DNA Multi-hairpin Motif

Lulu Zhang, Annie M. Bluhm,<sup>‡</sup> Kuan-Jen Chen,<sup>‡</sup> Nicholas E. Larkey,<sup>‡</sup> and Sean M. Burrows\*

Department of Chemistry, Oregon State University, 153 Gilbert Hall, Corvallis, Oregon 97331, United States.

**KEYWORDS:** Toe-hold, Branch Migration, Selectivity, Förster Resonance Energy Transfer, RNA, Thermodynamics, and Crude cell lysate.

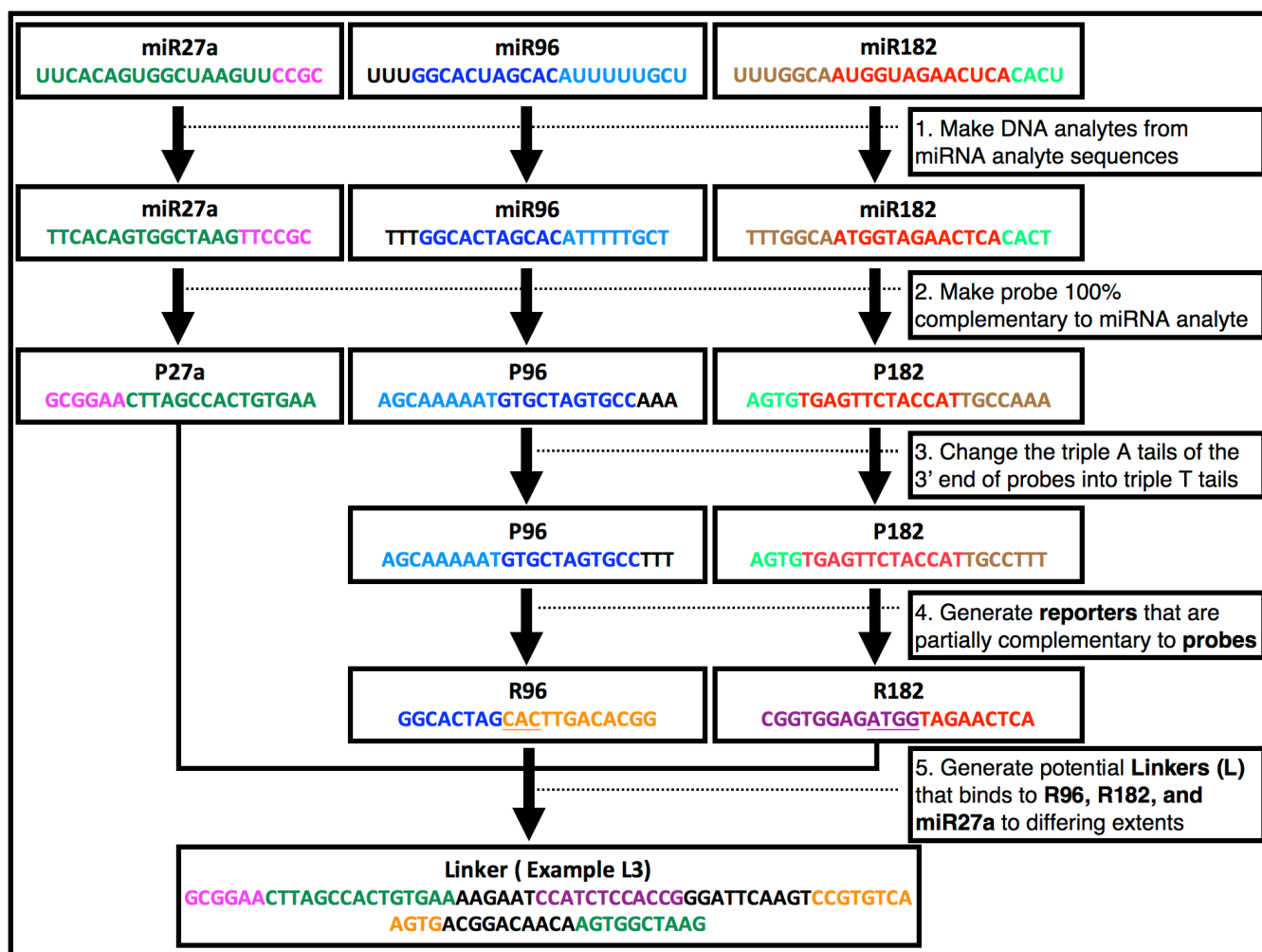


**Figure S1.** The flow chart of the nano-assembly logic gate design process. Matching colors indicate complementary base pairs. Mismatched colors indicate non-complementary base pairs.

## **Section 1: Reporter and Linker filtration process.**

The Matlab program produced hundreds to thousands of potential reporters and linkers. These reporter candidates were filtered to rule out those having cross reactivity with off-analyte nucleic acids (other miRs, mRNA, etc.), non-corresponding probes, non-corresponding regions on the linker, and other reporter strands. The evaluation of cross reactivity was based on the thermodynamic estimates by using the “Two-state melting (Hybridization)” (TSM) function from the DINAMelt Web Server.

A similar Matlab filtering process for the reporters was applied to the linkers. To fulfill the many requirements an ideal linker should be, the computer generated linkers had to go through a similar but more complicated filtration process than the reporters did. The linker filtering process includes: 1) estimating the secondary structure and thermodynamics of the multi-hairpin linker through “Quikfold” function (Table S5. A), 2) evaluating the off-analyte cross reactivity with the multi-hairpin linker through the TSM function (results in Table S6-S8), 3) evaluating the analyte (miR27a, R182, and R96) binding thermodynamic data through the TSM function (results in Table S6-S8), 4) evaluating the molar fraction of the logic circuits ON state formed when single, double, and all three analytes were present through “Hybridization of two different strands” function (Figure S5, S6), 5) comparing the probability of forming intramolecular hairpin secondary structure and intermolecular homodimer structure through “Homodimer Stimulations” function (no data shown), and 6) analyzing the number of H-bonds formed in the linker’s intramolecular hairpin secondary structure and between linker and analyte/off-analytes (Table S5. C-F). All the functions mentioned above were from the DINAMelt Web Server and the following settings were used: hybridization temperature of 37 °C, Na<sup>+</sup> concentration of 10 mM, Mg<sup>2+</sup> concentration of 2.5 mM, and strand concentration of 100 nM.

L0	5'- GCGGAACTTAGCCACTGTGAA CGAAAGCCCTGATCTCCAGCATTAGGG CTTTATGGCCTTGTTTTGTGAATGCAAGGCCATAACGTTACAGTGGC-3'
L1	5'- GCGGAACTTAGCCACTGTGAA GATATCGCCATCTCCACCGATATCAAGT CCGTGTCAAGTGACGGACAAACAGTGGCTAA-3'
L2	5'- GCGGAACTTAGCCACTGTGAA AAGAATCCATCTCCACCGGGATTCAAGT CCGTGTCAAGTGACGGACAACAAGTGGCTAA-3'
L3	5'- GCGGAACTTAGCCACTGTGAA AAGAATCCATCTCCACCGGGATTCAAGT CCGTGTCAAGTGACGGACAACAAGTGGCTAAG-3'
L4	5'- GCGGAACTTAGCCACTGTGAA GATATCGCCATCTCCACCGATATCAAGT CCGTGTCAAGTGACGGACAACACAGTGGCTAAG-3'
L5	5'- GCGGAACTTAGCCACTGTGAA GATATCGCCATCTCCACCGATATCAAGT CCGTGTCAAGTGACGGACAAACAGTGGCTAAG-3'

**Table S1.** The linkers' sequences. The sequences (from 5' to 3') in blue, purple, and orange were binding regions for miR27a (HS-27a), R182 (HR-182), and R96 (HR-96) respectively.

miR27a	5'-TTCACAGTGGCTAAGTTCCGC-3'
miR96	5'-TTTGGCACTAGCACATTTTGTGCT-3'
miR182	5'-TTTGGCAATGGTAGAACTCACACT-3'
R96 for L1 to L5	5'-GGCACTAGCACTTGACACGG/iSpC3//iSpC3//36-FAM/-3'
R182 for L1 to L5	5'-/5ATTO633N//iSpC3//iSpC3/CGGTGGAGATGGTAGAACTCA-3'
P96	5'-AGCAAAAATGTGCTAGTGCCTTT-3'
P182	5'-AGTGTGAGTTCTACCATTGCCTTT-3'
R96 for L0	5'-/5BiotinTEG/TTTGGCACTAGCACAAAACAAGG/iSpC3//36-FAM/-3'
R182 for L0	5'-/5ATTO633N//iSpC3/AATGCTGGAGGGTAGAACTCACACT/3BioTEG-3'

**Table S2.** The sequences of analyte miRs, probes, and reporters.

mmu-miR29b-1-5p	5'-GCTGGTTTCATATGGTGGTTTA-3'
mmu-miR26a-2-3p	5'-CCTGTTCTTGATTACTTGTTTC-3'
hsa-miR146a-3p	5'-CCTCTGAAATTCAGTTCTTCAG-3'
hsa-miR146a-5p	5'-TGAGAACTGAATTCCATGGGTT-3'
hsa-miR146b-5p	5'-TGAGAACTGAATTCCATAGGCT-3'

**Table S3.** The sequences of off-analytes used to make off-analyte cocktail.

A

miR	miR	$\Delta G$	$\Delta H$	$\Delta S$	$T_m$
miR27a	miR27a	-3.0	-51.1	-155.1	-0.2
miR96	miR96	-2.5	-32.9	-97.9	-20.0
miR182	miR182	-3.4	-41.3	-122.1	-5.1
miR27a	miR96	-3.3	-32.6	-94.5	-21.0
miR27a	miR182	-3.4	-31.6	-90.9	-21.7
miR96	miR182	-4.3	-72.3	-219.4	11.3

B

Probe	miR	$\Delta G$	$\Delta H$	$\Delta S$	$T_m$
P96	miR27a	-3.6	-37.8	-110.3	-12.6
P96	miR96	-21.7	-165.3	-463.1	58.9
P96	miR182	-4.3	-43.8	-127.3	-3.0
P182	miR27a	-3.6	-37.8	-110.3	-12.6
P182	miR96	-3.9	-38.5	-111.6	-10.2
P182	miR182	-22.3	-171.1	-479.7	59.4

C

Reporter	miR	$\Delta G$	$\Delta H$	$\Delta S$	$T_m$
R96	miR27a	-3.3	-32.6	-94.5	-21.0
R96	miR96	-3.0	-32.9	-96.6	-22.7
R96	miR182	-3.6	-42.1	-124.0	-8.1
R182	miR27a	-3.4	-31.6	-90.9	-21.7
R182	miR96	-3.6	-42.1	-124.0	-8.1
R182	miR182	-3.1	-34.0	-99.7	-20.3

D

Reporter	Probe	$\Delta G$	$\Delta H$	$\Delta S$	$T_m$
R96	P96	-12.6	-99.3	-279.4	42.9
R96	P182	-3.4	-33.6	-97.5	-19.1
R182	P96	-2.1	-25.1	-74.3	-43.1
R182	P182	-11.6	-117.6	-341.6	39.3

E

Reporter	miR	$\Delta G$	$\Delta H$	$\Delta S$	$T_m$
R96	miR27a	-3.3	-32.6	-94.5	-21.0
R96	miR96	-3.2	-45.9	-137.8	-7.2
R96	miR182	-3.6	-42.1	-124.0	-8.1
R182	miR27a	-3.4	-31.6	-90.9	-21.7
R182	miR96	-3.9	-37.9	-109.5	-10.5
R182	miR182	-2.6	-35.8	-107.0	-20.7

F

Reporter	Probe	$\Delta G$	$\Delta H$	$\Delta S$	$T_m$
R96	P96	-13.8	-103.8	-290.0	46.4
R96	P182	-3.9	-38.5	-111.6	-10.2
R182	P96	-3.2	-35.7	-104.9	-17.6
R182	P182	-14.9	-120.9	-341.8	47.9

**Table S4.** Estimated thermodynamic data of cross reactivity between three miRs (A), probes with miRs (B), reporters for L1-5 with miRs (C), and reporters for L1-5 with probes (D), reporters for L0 with miRs (E), reporters for L0 with probes (F). The “Two-State Melting (Hybridization)” (TSM) function from the free online software DINAMelt Server was used to estimate all thermodynamic data. The units for the free energy and enthalpy are kcal/mol, for entropy are cal/(mol\*K), for melting temperature is °C.

A	Multi-hairpin				
	L	$\Delta G$	$\Delta H$	$\Delta S$	$T_m$
	0	-24.35	-240.1	-695.66	72.0
	1	-14.14	-194.7	-582.17	61.3
	2	-10.16	-169.2	-512.78	56.8
	3	-12.15	-185.5	-558.92	58.7
	4	-18.5	-228.7	-677.43	64.3
	5	-16.13	-211.0	-628.31	62.7

B	Intermolecular dimer				
	L	$\Delta G$	$\Delta H$	$\Delta S$	$T_m$
	0	-36.5	-379.4	-1105.7	60.3
	1	-11.6	-284.4	-879.6	38.8
	2	-8.7	-109.2	-324.0	33.6
	3	-9.8	-78.5	-221.4	36.6
	4	-20.5	-317.4	-957.2	47.7
	5	-15.6	-317.4	-971.8	42.6

C	R96		R182	
	L0	Total bases GC pairs	Total bases GC pairs	
	P96	127	/	/
	P182	/	157	

D	R96		R182	
	L1-5	Total bases GC pairs	Total bases GC pairs	
	P96	117	/	/
	P182	/	157	

E	R96		R182		miR27a	
	L	Total bases GC pairs	Total bases GC pairs		Total bases GC pairs	
	0	125	105		2111	
	1-5	127	128		2111	

F	HR-182		HR-96		HS-27a	
	L	Total bases GC pairs	Total bases GC pairs		Total bases GC pairs	
	0	74	95		138	
	1	73	64		115	
	2	63	64		94	
	3	63	64		105	
	4	73	64		137	
	5	73	64		126	

**Table S5.** Linker's estimated thermodynamic data for multi-hairpin structure (A) and intermolecular homodimer structure (B), number of base pairs (total and GC) between reporters for L0 and probes (C), number of base pairs (total and GC) between reporters for L1-5 and probes (D), number of base pairs (total and GC) between reporters/miR27a and linkers (E), and number of base pairs (total and GC) for the stem parts of HR-182, HR-96, and HS-27a of the linkers (F). The “Quikfold” and TSM functions from the free online software DINAMelt Server were used to estimate all thermodynamic data.

Estimated thermodynamic data		$\Delta G$	$\Delta H$	$\Delta S$	$T_m$
GCGGAACTTAGCCACTGTGAACGAAAGCCCTGATCTCCAGCATTAGGGCTT TATGGCCTTGTTTTGTGAATGCAAGGCCATAACGTTACAGTGGC;					
miR27a	TTCACAGTGGCTAAGTTCCGC;	-23.0	-165.2	-458.4	61.8
R96	TTTGGCACTAGCACAAAACAAGG;	-12.3	-101.8	-288.7	41.6
R182	AATGCTGGAGGGTAGAACTCACACT;	-10.1	-79.9	-225.0	34.4
miR96	TTTGGCACTAGCACATTTTTTGCT;	-4.2	-38.0	-109.1	-9.1
miR182	TTTGGCAATGGTAGAACTCACACT;	-4.2	-38.0	-109.1	-9.1
P96	AGCAAAAATGTGCTAGTGCCTTT;	-4.8	-35.1	-97.7	-8.3
P182	AGTGTGAGTTCTACCATTGCCTTT;	-4.8	-35.1	-97.7	-8.3

**Table S6.** Estimated thermodynamic data of hybridization between L0 and other single-strand DNAs at 37 °C. Two-state melting (Hybridization) (TSM) from the DINAMelt Web Server was used to estimate double-strand hybridization thermodynamic values of the linkers binding with any of the three miRs and two probe strands, finding no favorable binding with the linker. The fact there was no favorable binding meant less cross reactivity between miRs, probes, and linkers.

Estimated thermodynamic data		$\Delta G$	$\Delta H$	$\Delta S$	$T_m$
GCGGAACTTAGCCACTGTGAAGATATCGCCATCTCCACCGATATCAAGTC CGTGTCAAGTGACGGACAAACAGTGGCTAA;					
miR27a	TTCACAGTGGCTAAGTTCCGC;	-23.0	-165.2	-458.4	61.8
R96	GGCACTAGCACTTGACACGG;	-14.0	-104.2	-290.7	47.0
R182	CGGTGGAGATGGTAGAACTCA;	-14.3	-102.8	-285.2	48.1
miR96	TTTGGCACTAGCACATTTTTTGCT;	-4.2	-38.0	-109.1	-9.1
miR182	TTTGGCAATGGTAGAACTCACACT;	-4.2	-38.0	-109.1	-9.1
P96	AGCAAAAATGTGCTAGTGCCTTT;	-3.6	-37.8	-110.3	-12.6
P182	AGTGTGAGTTCTACCATTGCCTTT;	-3.8	-37.2	-107.7	-12.0

**Table S7.** Estimated thermodynamic data of hybridization between L1 and other single-strand DNAs at 37 °C. Two-state melting (Hybridization) (TSM) from the DINAMelt Web Server was used to estimate double-strand hybridization thermodynamic values of the linkers binding with any of the three miRs and two probe strands, finding no

favorable binding with the linker. The fact there was no favorable binding meant less cross reactivity between miRs, probes, and linkers.

Estimated thermodynamic data		$\Delta G$	$\Delta H$	$\Delta S$	$T_m$
GCGGAACTTAGCCACTGTGAAAAGAATCCATCTCCACCGGGATTCAAGTC CGTGTCAAGTGACGGACAACAAGTGGCTAAG;					
miR27a	TTCACAGTGGCTAAGTTCCGC;	-23.1	-165.5	-459.9	61.8
R96	GGCACTAGCACTTGACACGG;	-14.0	-104.2	-290.7	47.0
R182	CGGTGGAGATGGTAGAACTCA;	-13.7	-103.5	-289.5	46.0
miR96	TTTGGCACTAGCACATTTTGTCT;	-4.2	-38.0	-109.1	-9.1
miR182	TTTGGCAATGGTAGAACTCACACT;	-4.2	-38.0	-109.1	-9.1
P96	AGCAAAAATGTGCTAGTGCCTTT;	-3.6	-37.8	-110.3	-12.6
P182	AGTGTGAGTTCTACCATTGCCTTT;	-3.8	-37.2	-107.7	-12.0

**Table S8.** Estimated thermodynamic data of hybridization between L3 and other single-strand DNAs at 37 °C. Two-state melting (Hybridization) (TSM) from the DINAMelt Web Server was used to estimate double-strand hybridization thermodynamic values of the linkers binding with any of the three miRs and two probe strands, finding no favorable binding with the linker. The fact there was no favorable binding meant less cross reactivity between miRs, probes, and linkers.

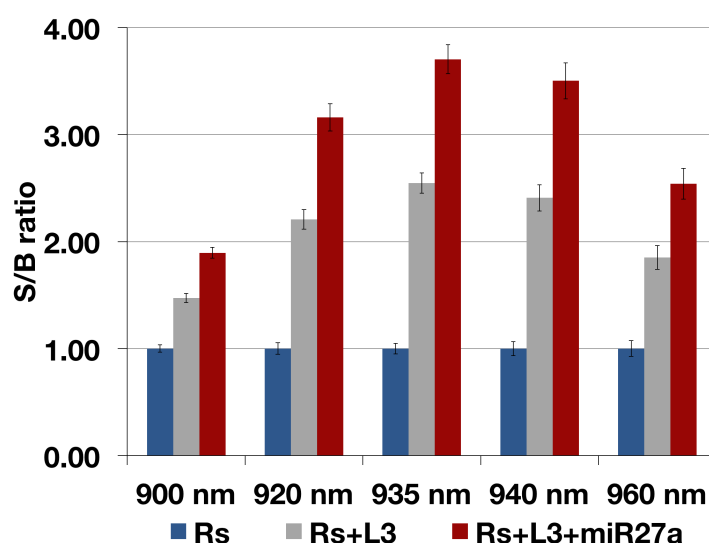


**Figure S2.** The excitation wavelength determination. When excited at 935 nm, L3 showed the highest signal to background (S/B) ratio (N = 2). The acquisition settings were the same as described in experimental section except the exposure time was 250 ms.



## Section 2: FRET Efficiency and FRET Distance Calculations

The distance between the dyes, FAM and ATTO 633, on two different linkers, L1 and L3 were estimated using the following two equations:

$$E = 1 - \left( \frac{I_{DA}}{I_D} \right) \text{ and } r = R_0 \sqrt[6]{\frac{1-E}{E}}.$$

With the first equation,  $I_{DA}$  was the emission intensity of FAM when all miRs were added to a solution with RP182, RP96, and the linkers.  $I_D$  was the emission intensity of the FAM-RP96 when it was in the presence of ATTO 633-RP182, but in the absence of the linker and all miRs. There were equal concentrations of FAM-DNA to ATTO 633-DNA in both  $I_D$  and  $I_{DA}$  samples. All samples were excited at 935 nm.

To ensure the ATTO 633 did not influence the FAM signal we measured FAM signal with and without ATTO 633 present. The emission intensity of FAM alone was similar to that when FAM was mixed with ATTO 633 (no data shown). Thus, the presence of ATTO 633 did not significantly influence the signal from FAM.

The average E value was then used in the second equation to calculate the distance between FAM and ATTO 633. A literature value of the Förster distance,  $R_0$ , for the FAM and ATTO 633 pair was not available in the literature. However, an  $R_0$  value of 51 Å for the ATTO 488 and ATTO 633 pair was available. This  $R_0$  value was used because FAM and ATTO 488 have similar emission wavelengths near 520 nm. For L3, E was found to be  $0.2647 \pm 0.0022$ . With the estimated  $R_0$  value and the calculated E value for L3, r was calculated to be 60.49 Å. For L1, E was found to be  $0.2722 \pm 0.0024$  and the distance between the FRET pair, r, was found to be 60.08 Å.

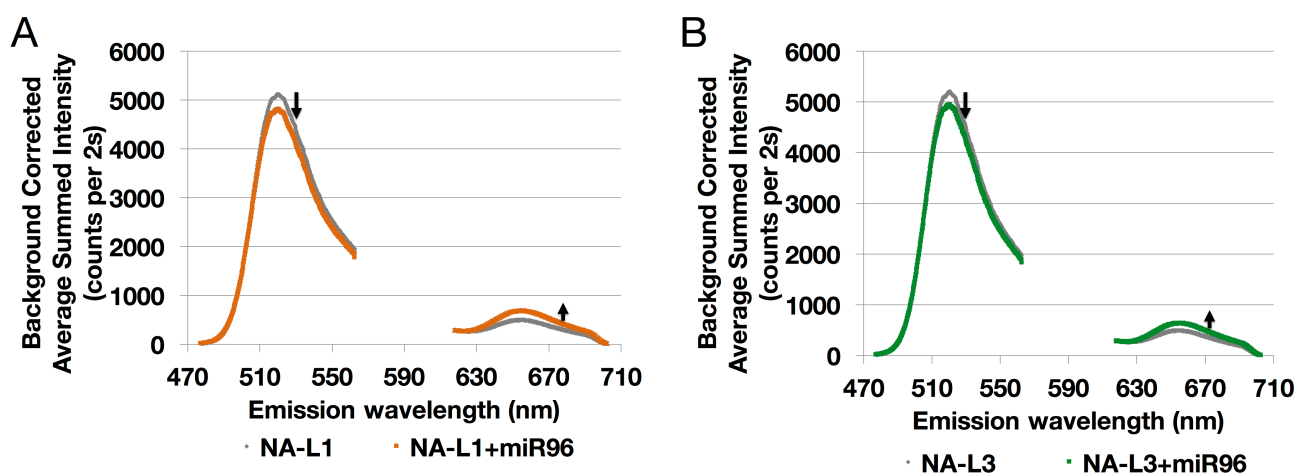


**Figure S3.** The emission spectrum from adding miR96 to NA-L1 (A) and NA-L3 (B) (N = 3).

### Section 3: Comparison of Six Linkers: L0 to L5.

Figure S4 shows that for each linker, the presence of both reporters caused the R/G ratio to increase by about 3 times (Rs+L, gray bar) compared to the control group of two reporters (Rs, blue bar). When both reporters with miR27a were added to each linker, all the linkers showed the R/G ratio increased by about 5 times (Rs+L+miR27a, red bar) compared to the control group of two reporters (Rs, blue bar).

There were no statistically significant differences between the five linkers as to their responses towards either two reporters, or two reporters with miR27a. L1 and L3 were chosen as representative linkers for further tests.

Amongst L1-L5 there were some nuanced differences between the stem's sequence and thermodynamics for HR-182. However, the stem's sequence and thermodynamics for HR-96 were the same. These nuanced differences in the sequence might be the reason for the similar response toward to the addition of R96 and R182 (Rs) with and without miR27a (Figure S4).

The sequences for L1, L4, and L5 were almost the same except for the last 12-13 nucleotides in the 3' end. L5 has one more guanine base at the 3' end than L1. L4 has one more cytosine base than L5. L2 and L3 had similar sequences, but L3 had one more guanine base at the end of 3', making it more thermodynamically stable than L2. The HR-182 of the five linkers was mostly similar in the stem sequence and energy. L1, L4, and L5 all had the same HR-182 sequences with Gibbs energy of -2.2 kcal/mol. L2 and L3 had the same HR-182 sequences with Gibbs energy of about -1.9 kcal/mole. The hairpin region HR-96 had the same stem sequence for L1 to L5. Thus the stabilities of HR-182 and HR-96 were quite similar for L1 to L5. These similarities in the HRs resulted in the similar response towards to the addition of R96 and R182 (Rs) (Figure S4).

Compared to L1-L5, L0 failed to respond to two Rs with or without miR27a. This result can be explained by the estimated thermodynamic data. For L0, the Gibbs energies for HR-182 and HR-96 were ~4 and ~7 kcal/mole, respectively. The hairpin region's stems in L0 were very different and more thermodynamically stable than those of L1-L5. The linker-reporter complexes' Gibbs energies for linker L0 were ~12 and ~10 for R96 and R182, respectively. Looking at the number of GC base pairs, there were 8 when R182 bound to L1-L5, but only 5 when R182 bound to L0. Also there were two more GC bases paired when R96 bound to L1-L5 than to L0 (Table S5. E). The linker reporter binding interactions were weaker for L0 than those for L1-L5. Even though L0's HS-27a had a similar stability to L4, and both were more stable than any other linker, L0 failed to respond to two Rs with the addition of miR27a.

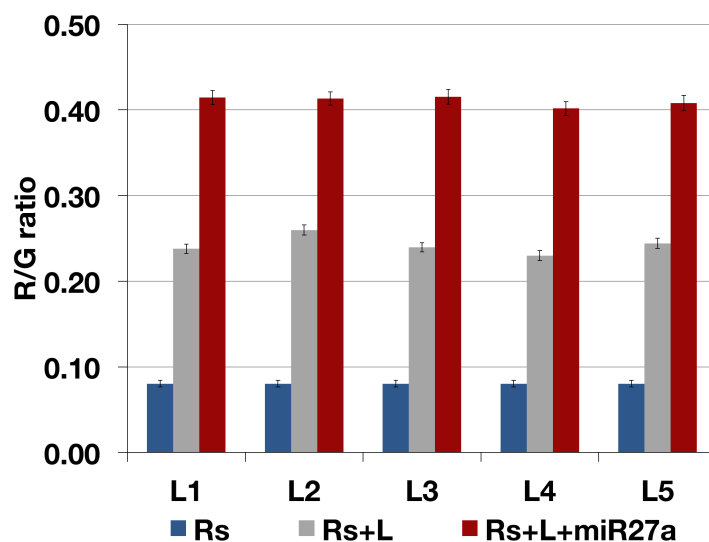


**Figure S4.** All five linkers showed similar response towards the addition of R96 and R182 (Rs) with and without miR27a (N = 2). The acquisition settings were the same as described in experimental section except the exposure time was 250 ms.

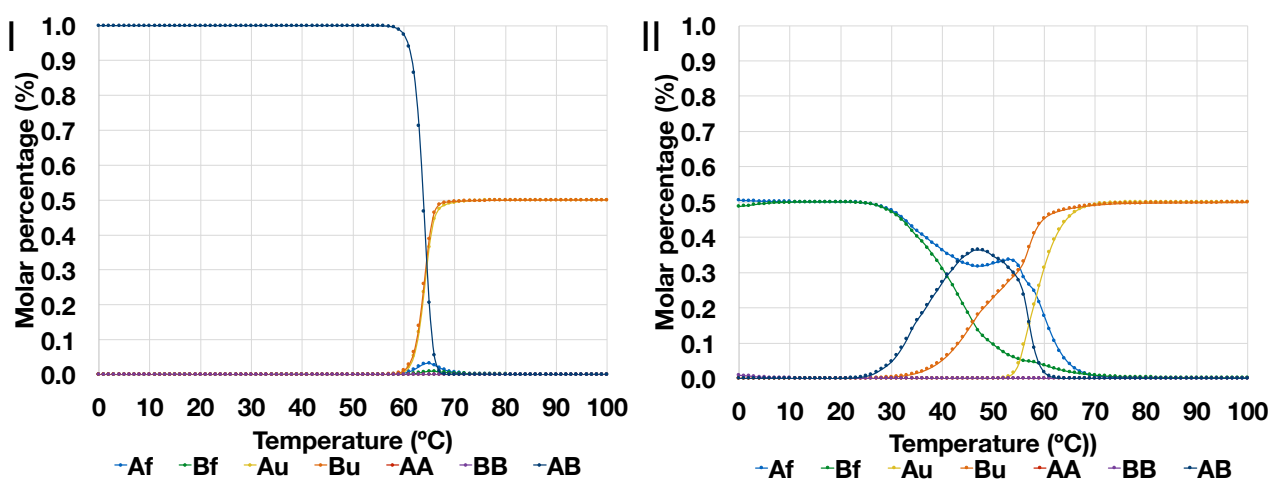


**Figure S5.** Estimated concentration when two DNA analytes were hybridized at different temperatures. In the figures A was L3 (for I and II), B was either R96-R182-miR27a (for I) or R96-R182 (for II), and the dashed line was the heterodimer concentration between A and B. The subscript f = folded, u = unfolded, AA and BB were homodimers, and AB was the heterodimer. (I) Showed almost 100 % binding of A and B strands when the hybridizing temperature was 37 °C, meaning R96, R182, and miR27a strongly bound to L3 at 37 °C. (II) Showed about 20% binding of A and B strands when the hybridized temperature was around 37 °C, showing R96 and R182 were able to bind to L3 at 37°C and was reflected in the experimental FRET data. The free online software DINAMelt was used to estimate all thermodynamic data; the function used here was “Hybridization of two different DNA strands” (model: Energy minimization).

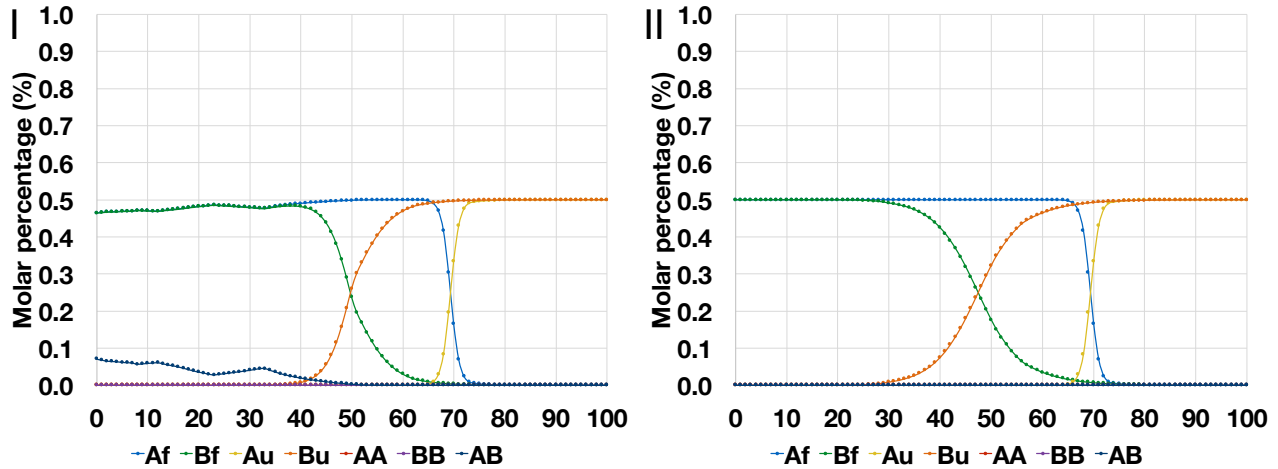


**Figure S6.** Estimated concentration when two DNA analytes were hybridized at different temperatures. In the figures A was L0 (for I and II), B was either R96-R182-miR27a (for I) or R96-R182 (for II), and the dashed line was the heterodimer concentration between A and B. The subscript f = folded, u = unfolded, AA and BB were homodimers, and AB was the heterodimer. (I) Showed 2.82 % binding of A and B strands when the hybridizing temperature was 37 °C, meaning R96, R182, and miR27a barely bound to L0 at 37 °C. (II) Showed 0 % binding of A and B strands when the hybridized temperature was around 37 °C, showing R96 and R182 were not able to bind to L0 at 37 °C. The fact L0 failed to bind both reporters and miR27a was reflected in the FRET data. The free online software DINAMelt was used to estimate all thermodynamic data; the function used here called “Hybridization of two different DNA strands” (model: Energy minimization).